Journal of Alloys and Compounds 505 (2010) L23–L26

Contents lists available at ScienceDirect

Journal of Alloys and Compounds

journal homepage: www.elsevier.com/locate/jallcom

Letter

Charge disproportionation in AlV_2O_4: A first-principles study

Yongmao Cai[a], Zu-Fei Huang[b], Xing Ming[b,c], Chunzhong Wang[b], Gang Chen[b,*]

[a] College of Materials Science and Engineering, Jilin University, Changchun 130012, People's Republic of China
[b] College of Physics/State Key Laboratory of Superhard Materials, Jilin University, Changchun 130012, People's Republic of China
[c] College of Physical Science and Technology, Huanggang Normal University, Huanggang 438000, People's Republic of China

ARTICLE INFO

Article history:
Received 23 November 2009
Received in revised form 16 June 2010
Accepted 22 June 2010
Available online 1 July 2010

Keywords:
First-principles calculation
Charge disproportionation
Heptamer
Rhombohedral AlV_2O_4

ABSTRACT

The charge disproportionation of V ions in the low-temperature rhombohedral phase of AlV_2O_4 has been studied by first-principles density functional theory (DFT) computations. The calculation results show that there exists an alone V ion (V1) and a "heptamer" constructed by two types of V ions (one V2 and six V3) in the rhombohedral AlV_2O_4. The theoretical results are consistent with previous experimental reports (Horibe et al., Phys. Rev. Lett. 96 (2006) 086406; Phys. Rev. Lett. 96 (2006) 169901). The valence states of the three types of V ions are found to be $+(2.5-\delta1)$, $+(2.5+\delta2)$ and $+(2.5+(\delta1-\delta2)/6)$ ($\delta1>\delta2>0$), respectively. The three types of V ions with different charges arrange periodically layer by layer along the *c*-axis direction with a sequence as V1–V3–V2–V3–V1.

1. Introduction

Transition metal compounds display abundant peculiar physical properties which have been confusing people a long time, such as the charge disproportionation or charge order of the transition metal [1–4], the colossal magnetoresistance [5–7], unconventional superconductivity [8], etc. The charge, spin, and orbital degrees of freedom of electron in transition metal compound are often strong coupled [9], which make the problem much complicated. Recently, AlV_2O_4, a new typical mixed valence compound, has attracted a lot of interest [10–16]. Previous experimental measurements show that AlV_2O_4 transforms from a high-temperature cubic phase to a low-temperature rhombohedral phase at 700 K [10,11]. Matsuno et al. proposed a three-one type charge ordering model: the $V^{2.5+}$ ions are separated into three $V^{(2.5-\delta)+}$ ions on the kagome lattices and one $V^{(2.5+3\delta)+}$ ion on the triangular lattices [10]. But this model cannot explain the presence of the superlattice structure revealed by both X-ray powder diffraction and electron diffraction. Horibe et al. examined the charge-ordered state in AlV_2O_4 carefully with electron diffraction and synchrotron X-ray diffraction [11]. They reported that in the low-temperature rhombohedral phase, there are three inequivalent V sites denoted as V1, V2 and V3 with their valence states being assumed to be +3 (d^2), +2 (d^3), and +2.5 ($d^{2.5}$), respectively, and a "heptamer" (i.e. a V cluster is composed of six V3 ions and one V2 ion) and an alone V1 ion order periodically. They explained the valence of "left-alone" V1 ion as trivalent, based on the V1–O bond length (2.044 Å) being close to the normal V^{3+}–O^{2-} bond length [11]. However, the V2–O bond length (2.024 Å) is shorter than the V1–O bond length. According to the bond valence method, those with lower valence are longer in the bond length and those with higher valence are shorter [17]. V2 should have a higher valence than V1, which is opposite to the assumption mentioned above. Therefore, the electronic structure of AlV_2O_4, especially the charge disproportionation of the V ions in the rhombohedral AlV_2O_4 is still ambiguous. In this letter, we study the charge disproportionation of V ions in the rhombohedral AlV_2O_4 by first-principles calculations, a method which has been proven to be very valid for charge ordering or charge disproportionation in transition metal oxides, such as Fe_3O_4 [18,19], $YNiO_3$ [20], etc.

2. Computational method

All first-principles calculations are performed with the CASTEP code [21] by using plane-wave basis sets and Vanderbilt ultrasoft pseudopotentials [22]. The number of plane waves in the basis is determined by a cut-off energy of 500 eV. The valence electrons considered in this study are Al ($3s^23p^1$), V ($3s^23p^63d^34s^2$) and O ($2s^22p^4$). The GGA with more accurate Wu-Cohen (WC) exchange functional [23] are used to describe the exchange and correlation potentials. The Wu-Cohen exchange functional is better at prediction of lattice parameter, crystal structures and metal surface energies than the most popular PBE-GGA [23]. The special *k*-points sampling integration over the Brillouin zone is employed by using the Monkhorst–Pack method [24] with a *k*-point separation of 0.04 $Å^{-1}$ and $5\times5\times5$ *k*-mesh.

The crystal structure of rhombohedral AlV_2O_4 is shown in Fig. 1 and the space group is *R*-3*m*. The lattice parameters of the primitive cell are $a=b=c=10.175$ Å, based on the rhombohedral notation. The detailed fractional coordinates can be found elsewhere [11]. The calculated model structure consists of four AlV_2O_4 chemical formulas. To test the validity of calculations, we first optimize the geometry

* Corresponding author. Tel.: +86 431 85167336; fax: +86 431 85167336.
E-mail address: gchen@jlu.edu.cn (G. Chen).

0925-8388/$ – see front matter © 2010 Elsevier B.V. All rights reserved.
doi:10.1016/j.jallcom.2010.06.130

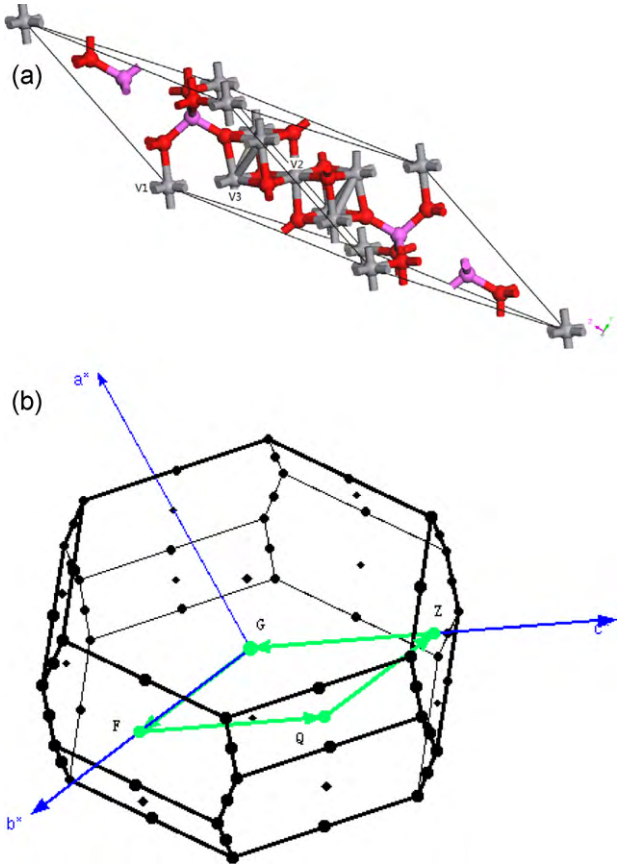

Fig. 1. (a) Crystal structure of low-temperature rhombohedral phase of AlV_2O_4. V1, V2 and V3 denote the three inequivalent V sites. (b) The corresponding Brillouin zone as well as its highly symmetrical special *k* points.

of AlV_2O_4 using the GGA method. Then the electronic structures of rhombohedral AlV_2O_4 are calculated based on the optimized structure. When calculating electronic structure, we have set up both non-magnetic and magnetic structures. In the magnetic states calculations, we suppose that each V ion has two d electrons. The initial magnetic moments of (V1, V2, V3) are set artificially as (−2, −2, 2), (2, −2, 2), (2, 2, 2), and (−2, 2, 2)μ_B, which are denoted as M1, M2, M3 and M4, respectively. Then the magnetic moments of V ions in the rhombohedral AlV_2O_4 are optimized by self-consistent calculations.

3. Results and discussion

The calculated structural parameters together with experimental parameters are shown in Table 1. The theoretically calculated lattice parameters fit well with the experimental value. The calculated characteristics of the structural distortion are shown in Fig. 2.

Table 1
Calculated and experimental lattice parameters, V–V bond lengths, average V-O bond lengths in the [VO_6] octahedra. V3–V3(l) and V3–V3(s) represent long and short V3–V3 bond length in the V3 layer, respectively.

		Cal.	Exp. [11]
a(=*b*=*c*) (Å)		10.008	10.175
Alpha		33.18	32.83
V (Å^3)		275.534	267.151
Bond lengths (Å)	V1–V3	3.021	3.039
	V2–V3	2.751	2.809
	V3–V3(l)	3.225	3.141
	V3–V3(s)	2.489	2.610
	V1–O	2.047	2.044
	V2–O	2.009	2.024
	V3–O	2.043	2.064

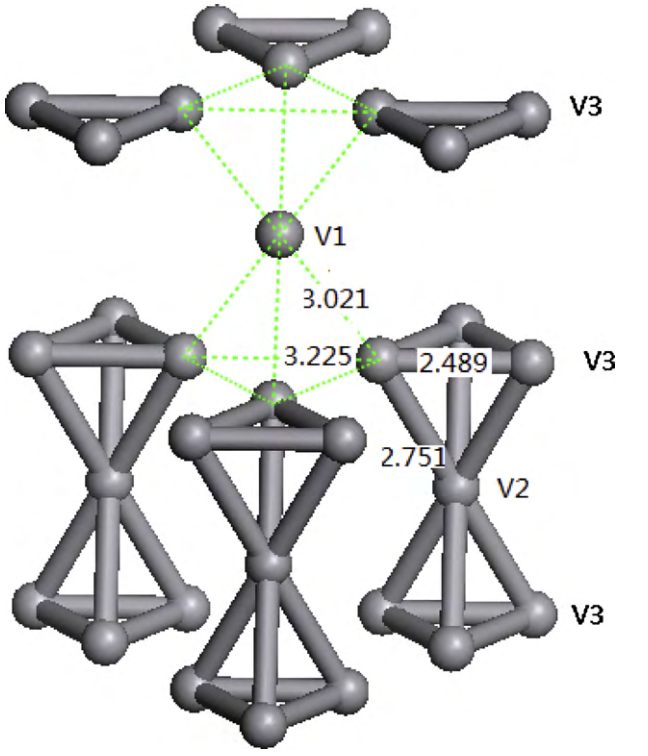

Fig. 2. Calculated V skeleton in rhombohedral AlV_2O_4. A "heptamer" constructed by one V2 and six V3 can be seen clearly.

Clearly, there are two kinds of V ions (V1, V2) on the triangular lattice, and one kind of V ion (V3) on the kagome lattice with two kinds of V3–V3 bonds in the V3 layer (the long V3–V3 bond and short V3–V3 bond denoted as V3–V3(l) and V3–V3(s)). Three V3 ions form the V3-trimers with short V3–V3(s) bond length (2.489 Å), which is much shorter than the long V3–V3(l) bond length (3.225 Å). Additionally, V2–V3 bond length (2.751 Å) is also much shorter than the V1–V3 bond length (3.021 Å) and all the V2 ions are sandwiched by two V3-trimers. Therefore, based on the V–V bond lengths, a V "heptamer" constructed by one V2 and six V3 can be found (see Fig. 2) in the rhombohedral AlV_2O_4, consistent well with previous experimental report [11].

The V magnetic moments and total energies of the four magnetic structures, together with energy of non-magnetic structure calculated by GGA are shown in Table 2. From Table 2, we can clearly see that the magnetic moments of V3 ion is very small (<0.2 μ_B). The four initial magnetic structures are relaxed into two magnetic structures M1 and M4. The total energy of M4 is just a little larger than M1 with a difference of 1.307 meV per formula unit (f.u.), so the magnetic structure M1 is used when calculating the electronic structure of AlV_2O_4. These results indicate that the V3 ions show paramagnetic behavior and the magnetic exchange coupling between V1 and V2 is pretty small. The calcu-

Table 2
Magnetic structures of AlV_2O_4 and their total energies per formula unit (energy of M1 is set to 0 meV) together with that of non-magnetic state.

	Magnetic moments of (V1, V2, V3) (μ_B)		Energy (meV/f.u.)
	Input	Output	
M1	(−2, −2, 2)	(−2.48, −1.76, 0.04)	0
M2	(2, −2, 2)	(2.44, −1.46, −0.16)	1.307
M3	(2, 2, 2)	(2.48, 1.76, −0.04)	−0.004
M4	(−2, 2, 2)	(−2.44, 1.76, 0.16)	1.310
NM	–	–	244.732

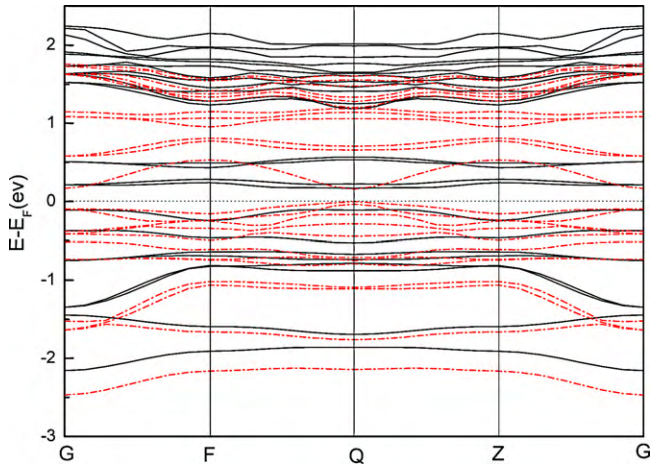

Fig. 3. The spin-polarized band structure of rhombohedral AlV_2O_4. The spin up/down subbands are plotted with solid/dotted lines.

lated results also indicate the magnetic solution has much lower energy than non-magnetic one with the total energy difference with 244.732 meV/f.u.

Revealed by the calculated band structures, the non-magnetic GGA calculation predicts a metallic character, which does not coincide with the experimental result [10], This result indicates that the magnetic structure of AlV_2O_4 should be considered adequately. Then we calculate the electronic structure of AlV_2O_4 with the M1 magnetic structure. A small band gap of 0.2 eV opens up (see Fig. 3), which agrees well with the experiment results and confirms the validity of the calculations again. The special *k* points and the *k*-path in the band structure can be seen Fig. 1(b). The bands are quite flat near the Fermi level (0 eV), indicating large density of states near the Fermi energy and strongly enhanced effective mass of the V-3d electrons.

In order to understand the detailed electronic structure of the three types of V ions and explore the charge distribution among the V ions, we plot the partial density of states (PDOS) around the Fermi level of V-3d and O-2p states. The PDOS calculations using CASTEP are based on Mulliken population analysis, which allows one to calculate the contribution from each energy band to a given atomic orbital. The distance cut-off for bond population was 3.0 Å. It is widely accepted that the absolute magnitude of the atomic charges yielded by population analysis have little physical meaning, for they display a high degree of sensitivity to the used atomic basis set [25]. However, their relative values can give useful information, provided that a consistent basis set is used for their calculation [26]. As shown in Fig. 4, the states below Fermi level can be divided into two parts: PART I from −10 to −4 eV and PART II from −2.5 eV to Fermi level.

According to the crystal field theory, in the octahedral crystal field the d-orbitals split into two sets of three t_{2g} and two e_g orbitals. Combined the band structures shown in Fig. 3, one can find from Fig. 4 that PART I is composed of 96 bands, where V e_g states and O-2p states form σ-type bonds. In a strongly ionic bond model, the antibonding band mainly consists of the V e_g states, while the bonding counterpart is mainly derived from O-2p states. This picture suggests that all the spin-polarized O-2p bands of all the 16 O atoms are occupied and the valence states of O atoms can be deduced reasonably to be −2. Similarly, PART II composed of 20 bands is V-3d t_{2g} states with only a few O-2p states. In PART II, where V-3d t_{2g} states point away from the oxygen, forms a set of nonbonding t_{2g} bands where the metal-metal interaction plays important role in its band width. The calculated electronic structures of AlV_2O_4 are typical of early transition metal oxides. The contributions of Al PDOS and V-4s PDOS to both PART I and PART II are little, suggesting an ionic behavior of Al^{3+} ion and the entire transfer of the V-4s electrons to the O-2p orbitals. Therefore, the Al and O ions can be defined to be Al^{3+} and O^{2-}, and the average valence of V ions is +2.5, which means there are 20 V-3d electrons, consistent well with the 20 spin-polarized bands in PART II.

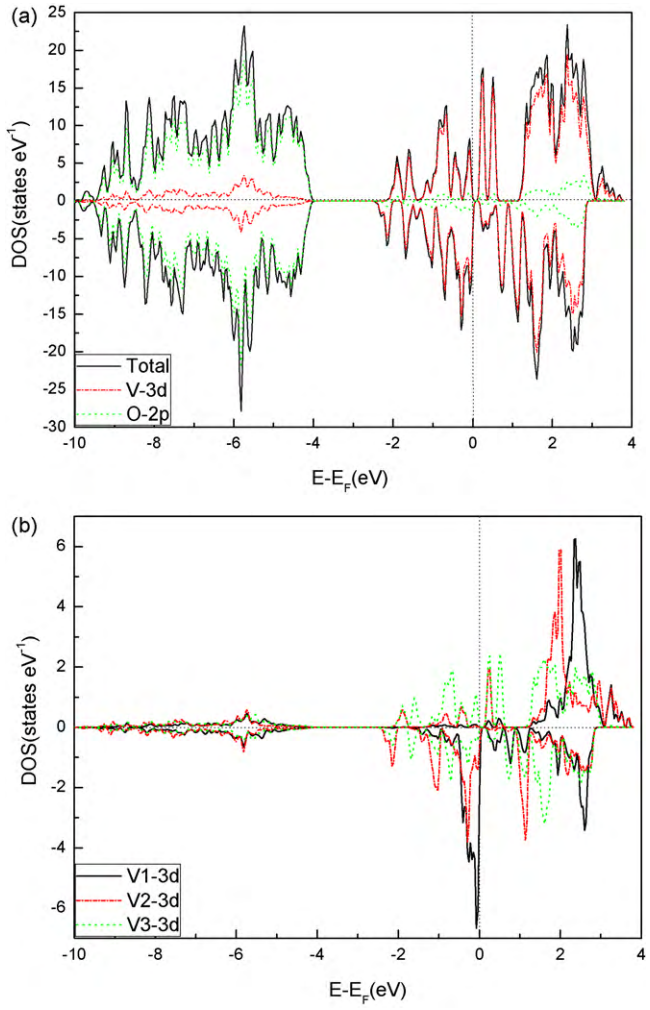

Fig. 4. Calculated partial density of states (PDOS). (a) V-3d and O-2p PDOS for all V and O atoms together with total DOS. (b) Detailed V-3d PDOS for each type of V atom.

Integration intensities of the three types of V-3d PDOS in both PART I and PART II are calculated and listed in Table 3. Previous reports have exposited that higher valence state for an atom corresponds to higher integration intensities in the PART I, which is bonding character. In contrast, due to the nonbonding character of PART II, higher valence state corresponds to lower integration

Table 3
Integration intensities of the three types of V-3d PDOS in rhombohedral AlV_2O_4, together with the charge disproportionation of V ions. Where, $\bar{V}$ is the average value.

Atom	PART I	PART II	Charge disproportionation of V ions ($\delta 1 > \delta 2 > 0$)
V1	1.17	2.26	$V^{(2.5-\delta 1)+}$
V2	1.30	2.19	$V^{(2.5+\delta 2)+}$
V3	1.28	2.19	$V^{(2.5+(\delta 1-\delta 2/6))+}$
$\bar{V}$	1.27	2.20	$V^{2.5+}$

intensities at PART II [20,27]. Therefore, it is natural that the calculated integration intensities of the 4 types of O-2p PDOS (not listed here) show little difference in both PART I and PART II, which indicates little difference in the valence states among the O ions in AlV_2O_4. From Table 3, compared to the average integration intensity, $\bar{V} = (V1 + V2 + 6V3)/8$ and corresponding to an valence state of +2.5, the integration intensities of V1 decrease by 0.10 in PART I and increase by 0.06 in PART II, which reveals the valence state of V1 ion is below +2.5, and it can be denoted as $+(2.5 - \delta 1)$. For V2 and V3 ions, the changes in the integration intensities are opposite to V1 ion. For the same analysis, the valence states of V2 and V3 ions are both above +2.5, and the valence state of V2 ion is a little higher than that of V3 ion. The valence state of V2 can be denoted as $+(2.5 + \delta 2)$, where $\delta 1 > \delta 2 > 0$ based on the difference between the integration intensities for V1 and V2 ions. According to the electric neutrality principle, the valence state of V3 can be assigned to be $+(2.5 + (\delta 1 - \delta 2)/6)$. So, among the three types of V ions, the valence of V1 is the lowest, V2 is the highest and V3 is the middle. The deviation from the formal valence is due to the covalency with neighbouring oxygen atoms, which is common for all transition metal oxides. Because the V1, V2 and V3 ions forms respective atom plane (as shown in Fig. 2), these V ions in rhombohedral AlV_2O_4 establish a charge ordering along the *c*-axis direction layer by layer with a sequence as $V1^{(2.5-\delta 1)+} - V3^{(2.5+(\delta 1-\delta 2/6))+} - V2^{(2.5+\delta 2)+} - V3^{(2.5+(\delta 1-\delta 2/6))+} - V1^{(2.5-\delta 1)+}$. The valence states, especially the relative magnitude for the three types of V ions are different from the results of Horibe et al. [11], i.e. V1 (V^{3+}), V2 (V^{2+}) and V3 ($V^{2.5+}$). Therefore, the model of the V "heptamer" with 18 electrons proposed by Horibe et al. [11] should be reconsidered and further experiments such as high-resolution XPS, resonant X-ray scattering and magnetic measurements are required to clarify the nature of the V "heptamer" in rhombohedral AlV_2O_4.

4. Conclusions

First-principles studies reveal that rhombohedral AlV_2O_4 has three types of V ions in the primitive cell: One alone V1, one V2 and six V3 ions, where the V2 and the six V3 ions construct a "heptamer". Calculated results indicate that charge disproportionations take place in these V ions with valence states of $+(2.5 - \delta 1)$, $+(2.5 + \delta 2)$ and $+(2.5 + (\delta 1 - \delta 2)/6)$ ($\delta 1 > \delta 2 > 0$), respectively, and form a charge ordering along the *c*-axis direction layer by layer with a sequence as V1–V3–V2–V3–V1.

Acknowledgments

This work was sponsored by the Special Funds for Major State Basic Research Project of China (grant no. 2009CB220104) and Program for Changjiang Scholar and Innovative Research Team in University (grant no. IRT0625). It is also supported by the Jilin Project of Research and Development (no. 20075007) and the Doctor Subject Foundation of China (grant no. 20070183003).

References

[1] E.J.W. Verwey, Nature 144 (1939) 327–328.
[2] J.E. Lorenzo, C. Mazzoli, N. Jaouen, C. Detlefs, D. Mannix, S. Grenier, Y. Joly, C. Marin, Phys. Rev. Lett. 101 (2008) 226401-1–226401-4.
[3] Hui Kong, Changfei Zhu, J. Alloys Compd. 478 (2009) 805–808.
[4] R.N. Bhowmik, R. Ranganathan, B. Ghosh, S. Kumar, S. Chattopadhyay, J. Alloys Compd. 456 (2008) 348–352.
[5] Y. Tokura, Rep. Prog. Phys. 69 (2006) 797–851.
[6] N. Ihzaz, M. Boudard, H. Vincent, M. Oumezzine, J. Alloys Compd. 479 (2009) 445–450.
[7] T. Tang, C. Tien, B.Y. Hou, J. Alloys Compd. 461 (2008) 42–47.
[8] J. AWilson, J. Phys.: Condens. Matter 22 (2010) 203201-1–203201-27.
[9] Y. Tokura, N. Nagaosa, Science 288 (2000) 462–468.
[10] K. Matsuno, T. Katsufuji, S. Mori, Y. Moritomo, A. Machida, E. Nishibori, M. Takata, M. Sakata, N. Yamamoto, H. Takagi, J. Phys. Soc. Jpn. 70 (2001) 1456–1459.
[11] Y. Horibe, M. Shingu, K. Kurushima, H. Ishibashi, N. Ikeda, K. Kato, Y. Motome, N. Furukawa, S. Mori, T. Katsufuji, Phys. Rev. Lett. 96 (2006) 086406-1–086406-4.
[12] Y. Horibe, M. Shingu, K. Kurushima, H. Ishibashi, N. Ikeda, K. Kato, Y. Motome, N. Furukawa, S. Mori, T. Katsufuji, Phys. Rev. Lett. 96 (2006) 169901–169911.
[13] K. Matsuno, T. Katsufuji, S. Mori, M. Nohara, A. Machida, Y. Moritomo, K. Kato, E. Nishibori, M. Takata, M. Sakata, K. Kitazawa, H. Takagi, Phys. Rev. Lett. 90 (2003) 096404-1–096404-4.
[14] A. Yaresko, I. Leonov, P. Fulde, Physica B 378 (2006) 1054–1055.
[15] K. Matsuda, N. Furukawa, Y. Motome, J. Phys. Soc. Jpn. 75 (2006), 124716-1r-r124716-7.
[16] Y. Shimizu, M. Tanaka, M. Itoh, T. Katsufuji, Phys. Rev. B 78 (2008) 144423-1–144423-6.
[17] I.D. Brown, The Chemical Bond in Inorganic Chemistry: the Bond Valence Model, Oxford Scientific Publications, Oxford, UK, 2002, p. 33.
[18] I. Leonov, A.N. Yaresko, V.N. Antonov, M.A. Korotin, V.I. Anisimov, Phys. Rev. Lett. 93 (2004) 146404-1–146404-4.
[19] H.T. Jeng, G.Y. Guo, D.J. Huang, Phys. Rev. Lett. 93 (2004) 156403-1–156403-4.
[20] X.G. Xu, X. Meng, C.Z. Wang, F. Wu, G. Chen, J. Phys. Chem. B 108 (2004) 1165–1167.
[21] S.J. Clark, M.D. Segall, C.J. Pickard, P.J. Hasnip, M.J. Probert, K. Refson, M.C. Payne, Z. Kristallogr. 220 (2005) 567–570.
[22] D. Vanderbilt, Phys. Rev. B 41 (1990) 7892–7895.
[23] Z. Wu, R.E. Cohen, Phys. Rev. B 73 (2006) 235116-1–235116-6.
[24] H.J. Monkhorst, J.D. Pack, Phys. Rev. B 13 (1976) 5188–5192.
[25] E.R. Davidson, S. Chakravorty, Theor. Chim. Acta 83 (1992) 319–330.
[26] M.D. Segall, R. Shah, C.J. Pickard, M.C. Payne, Phys. Rev. B 54 (1996) 16317–16320.
[27] X.G. Xu, C. Li, J.X. Li, U. Kolb, F. Wu, G. Chen, J. Phys. Chem. B 107 (2003) 11648–11651.